19

Rehabilitation of the Paralyzed Lower Limbs Using Functional Electrical Stimulation: Robust Closed Loop Control

Samer Mohammed, Philippe Poignet, Philippe Fraisse & David Guiraud
LIRMM – CNRS/INRIA – Université de Montpellier II
France

1. Introduction

The reliability, the ease of donning and doffing and the robustness of controllers constitute the primary criteria to evaluate any control strategy based on Functional Electrical Stimulation (FES). This technique is used to excite muscles that are under lesions and no more controlled by paraplegic patients. Consequently, the patient could recover partially some of its lower limb functions, improving the cardiovascular system and bettering the whole quality of life. Many FES based studies; both open loop and closed loop control showed satisfactory results in movement restoration. Although open loop control strategy induces excessive stimulation of the main muscles and consequently fast muscular fatigue, it is still adopted in most clinics till now. This could be explained mainly by their relative simple implantation (Bajd et al., 1981). Actually closed loop control strategies still have several drawbacks, such as overwhelming the patient by sensors' feedback, tuning the parameters of the controllers and identification for every patient, the lack of understanding the muscle contraction phenomena, etc. Closed loop controllers in FES context have been reported in many studies (Riener & Fuhr, 1998); (Mulder et al., 1992); (Donaldson & Yu, 1996). Some authors use a simple PID controller (Wood et al., 1998), Knee Extension Controller KEC (Poboroniuc et al., 2003), a combination of feedback and feed-forward control or an adaptive approach (Ferrarin et al., 2001). Others use a first or a second order switching curve in the state space to control patient movements: The On/Off controller (Mulder et al., 1992) and the ONZOFF controller (Poboroniuc et al., 2002), in the so-called "controller-centered" strategies. The main advantage of these strategies is their low number of parameters to be tuned during stimulation. The so-called "subject centered" strategies, (PDMR: Patient-Driven Motion Reinforcement (Riener & Fuhr, 1998), CHRELMS: Control by Handle REactions of Leg Muscle Stimulation (Donaldson & Yu, 1996)), introduce the voluntary contribution of the upper body of the patient as an essential part of the control diagram. This latter is not yet adopted in clinical use because of the relative high number of parameters to be identified. In order to overcome these drawbacks, we have applied two robust control strategies that are, the High Order Sliding Mode (HOSM) controller (Fridman & Levant, 2002) and the Model Predictive Controller (MPC) also known as receding horizon controller (Allgöwer et al., 1999). These controllers have been evaluated in simulation to highlight i) their performance in terms of capability of tracking a pre-defined reference trajectory and ii) the robustness against force perturbation and model mismatch. Furthermore the MPC technique constitutes an

Source: Rehabilitation Robotics, Book edited by Sashi S Kommu,
ISBN 978-3-902613-04-2, pp.648, August 2007, Itech Education and Publishing, Vienna, Austria

adequate controller for nonlinear multivariable systems and enables us to incorporate explicitly constraints on inputs, outputs and system states. The performances of these controllers have also been compared with a classical pole placement controller. The originality of the presented study comes also from the fact that these control strategies rely on the use of a physio-mathematical based muscle model. In fact, few studies have treated the human muscle as an entire physiological element in a control scheme. Some authors used linear muscle models; others represent the muscle as a non-linear function of recruitment with dynamics activation, angle and angular velocity dependence (Riener & Fuhr, 1998); (Veltink et al., 1992). The muscle model used in this study has been recently published (El-Makssoud et al., 2004-a) and it is based on a complex physio-mathematical formulation of the macroscopic Hill and microscopic Huxley concepts reflecting the dynamic phenomenon that occurred during muscle contraction and relaxation. In this model, the number of recruited motor units increases as a function of both the intensity and the pulse width of the stimulus. This phenomenon is modeled by an activation model (representing the ratio of recruited fibers). The contraction dynamics is expressed by a set of nonlinear differential equations representing the mechanical model. The goal of the present study is to represent the interaction between a closed loop controller and a closely physiological muscle model matching.

In next section, the system modeling is presented; it includes the knee-muscle biomechanical model, its state space formulation and parameter identification based on experimental setup. In the third and fourth sections, simulation results for controllers based on HOSM and MPC are presented. A comparison study of the controller performance is presented in the fifth section.

2. System modeling

Since closed loop control of different muscles actuating the knee joint of a paraplegic patient constitutes a prerequisite step before any upward mobility such as: standing up, standing, walking, climbing stairs, etc., we limited, in this stage, the study to a small scale biomechanical system. It consists of two segments representing respectively the shank and the thigh connected to each other by a revolute joint of one degree of freedom. The thigh is supposed to be fixed with respect to the patient while the shank is free to move around the knee joint (Fig.1). Two agonist/antagonist muscles act on the knee, the quadriceps acts as an extensor muscle while the hamstrings are the flexor muscle group. As a result two forces F_q and F_h cause respectively the extension and the flexion of the knee.

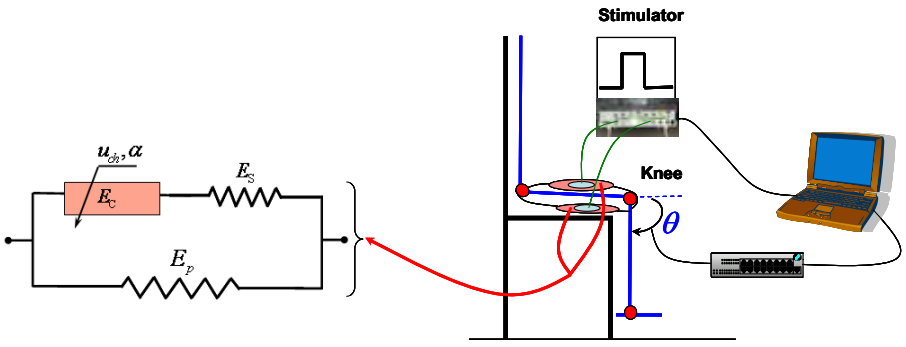

Fig. 1. Functional Electrical Stimulation applied to skeletal muscles.

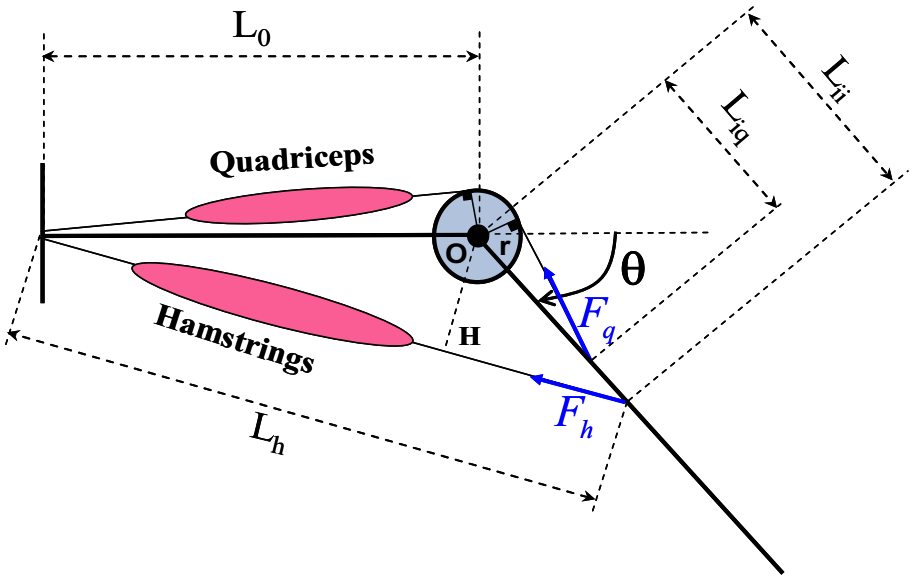

Fig. 2. Biomechanical model of the knee actuated by two groups of antagonistic muscles.

These forces are supposed to be constant along their directions on the whole corresponding muscle (Fig.2), (θ = 0 corresponds to full extension of the knee and θ = 90◦ represents the rest position). F_q and F_h are the inputs of the biomechanical model while the angle θ is the corresponding output. The geometric equations allow us to evaluate quadriceps length L_q depending on the knee angle variable theta:

$$L_q(\theta) = \sqrt{L_0^2 - r^2} + r\theta + \sqrt{L_{iq}^2 - r^2} \tag{1}$$

And the hamstrings length $L_h(\theta)$:

$$L_h(\theta) = \sqrt{L_0^2 + L_{ii}^2 + 2L_0 L_{ii}\cos(\theta)} \tag{2}$$

From the above equations, we can deduce the relative elongation of quadriceps and hamstrings.

$$\begin{aligned} \varepsilon_q(\theta) &= \frac{L_q - L_{0q}}{L_{0q}} = \frac{\sqrt{L_0^2 - r^2} + r\theta + \sqrt{L_{iq}^2 - r^2} - L_{0q}}{L_{0q}} \\ \varepsilon_h(\theta) &= \frac{L_h - L_{0h}}{L_{0h}} = \frac{\sqrt{L_0^2 + L_{ii}^2 + 2L_0 L_{ii}\cos(\theta)} - L_{0h}}{L_{0h}} \end{aligned} \tag{3}$$

L_{0q} and L_{0h} correspond respectively to the initial quadriceps and hamstrings lengths. Moment arm of the quadriceps is assumed to be constant and equal to the pulley radius r while the moment arm of the hamstrings depends on theta.

$$OH(\theta) = \frac{L_0 L_{ii} \sin(\theta)}{\sqrt{L_0^2 + L_{ii}^2 + 2L_0 L_{ii} \cos(\theta)}} \tag{4}$$

From the equations (3), (4) and the equation of motion that is a nonlinear second order equation, we obtained the acceleration $\ddot{\theta}$ (Eq. 5) as a function of the inertia about the knee joint I, gravity, joint damping factor F_v and joint elasticity K_e.

$$\ddot{\theta} = \frac{1}{I}\left[rF_q - mg\cos(\theta)\beta L_1 - K_e\theta - F_v\dot{\theta} - \frac{L_0 L_{ii}\sin(\theta)}{\sqrt{L_0^2 + L_{ii}^2 + 2L_0 L_{ii}\cos(\theta)}} F_h \right] \tag{5}$$

Identifications of the above parameters were performed based on experiments and are presented in the next section.

2.1 Muscle model

In previous papers (El-Makssoud et al., 2004-a; b), a physiological skeletal muscle model has been proposed to describe the complex internal physiological mechanism controlled by FES. In order to develop strategies for simulation, motion synthesis and motor control during clinical restoration of movement, we have adopted this model. In (Fig.3) we show the muscle model with the parallel element E_p representing the passive properties of the muscle and two elements in series: the serial element E_s and the contractile element E_c. This model is controlled by two variables: u_{ch}, a chemical control input and α the ratio of recruited fibers. This model has been described by two sets of differential equations (Eq.6) where the outputs are K_c and F_c representing, respectively, the stiffness and force generated by the contractile element. K_0 and F_0 are the maximum values of K_c and F_c. These equations could be expressed as follow:

$$\begin{cases} \dot{K}_c = \left(s_0\alpha k_0 - s_u K_c + s_v q \dfrac{s_0\alpha F_0 - s_u F_c}{1 + pK_c - s_v q F_c} K_c \right) u_{ch} - \dfrac{s_v a K_c}{1 + pK_c - s_v q F_c}\dot{\varepsilon} \\ \dot{F}_c = \dfrac{s_0\alpha F_0 - s_u F_c}{1 + pK_c - s_v q F_c} u_{ch} + \dfrac{bK_c - s_v a F_c}{1 + pK_c - s_v q F_c}\dot{\varepsilon} \end{cases} \tag{6}$$

$$s_u = sign(u_{ch}) = \begin{cases} -1 & if \quad u_{ch} < 0 \\ +1 & if \quad u_{ch} > 0 \end{cases} \qquad s_v = sign(\dot{\varepsilon}_c) = \begin{cases} +1 & if \quad \dot{\varepsilon}_c > 0 \\ -1 & if \quad \dot{\varepsilon}_c < 0 \end{cases} \tag{7}$$

$$\begin{gathered} s_0 = \frac{1+s_u}{2} \qquad a = \frac{L_0}{L_{c0}} \qquad b = L_0 \qquad p = \frac{1}{k_s} \qquad q = \frac{1}{L_{c0}k_s} \\ \varepsilon_c = \frac{L_c - L_{c0}}{L_{c0}} \qquad \varepsilon_s = \frac{L_s - L_{s0}}{L_{s0}} \qquad \varepsilon = \frac{L - L_0}{L_0} \qquad L = L_c + L_s \end{gathered} \tag{8}$$

Where s_u, and s_v are the sign functions related respectively to the control and velocities of the contractile element, L_c and L_s represent respectively the length of the contractile and the elastic elements. The ratio of recruited fibers α is considered as a global scale factor which gives the percentage of the maximal possible force that could be generated by the muscle.

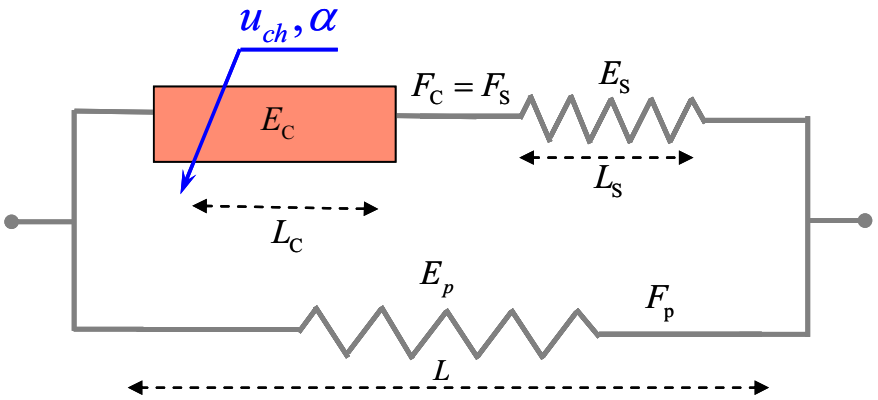

Fig. 3. Muscle model and particularity of E_c (El-Makssoud et al., 2004-a).

2.2 State space model of the muscles-knee

Let us consider the model of the muscles and knee joint as a non-linear state space model:

$$\dot{\mathbf{x}} = f(\mathbf{x}, \mathbf{t}, \mathbf{u}) \tag{9}$$

Where $\mathbf{x} = [x_1 \ldots x_6]^T = [K_{c_1} \quad K_{c_2} \quad F_{c_1} \quad F_{c_2} \quad \theta \quad \dot{\theta}]^T$ is the state vector while the control vector is expressed by $\mathbf{u} = [u_{q_{ch}} \quad \alpha_q \quad u_{h_{ch}} \quad \alpha_h]^T$. The variable θ represents the joint knee angle. The state variables K_{c1}, F_{c1}, u_{qch}, α_q and K_{c2}, F_{c2}, u_{hch}, α_h are respectively the state variables of the quadriceps and hamstrings. Consequently, the state representation of the biomechanical model (knee-muscles) could be expressed as:

$$\dot{x}_1 = \left(s_{0_1}\alpha_1 k_{0_1} - s_{u_1}x_1 + s_{v1}q_1 \frac{s_{0_1}\alpha_1 F_{0_1} - s_{u_1}x_3}{1 + p_1x_1 - s_{v_1}q_1x_3} x_1 \right) u_1 - \frac{s_{v_1}a_1x_1 r x_6}{L_{01}\left(1 + p_1x_1 - s_{v_1}q_1x_3\right)}$$

$$\dot{x}_2 = \left(s_{0_2}\alpha_2 k_{0_2} - s_{u_2}x_2 + s_{v_2}q_2 \frac{s_{0_2}\alpha_2 F_{0_2} - s_{u_2}x_4}{1 + p_2x_2 - s_{v_2}q_2x_4} x_2 \right) u_2 + \frac{s_{v_2}a_2x_2L_0L_{ii}\sin(x_5)}{L_{02}\sqrt{L_0^{\,2} + L_{ii}^{\,2} + 2L_0L_{ii}\cos(x_5)}\left(1 + p_2x_2 - s_{v_2}q_2x_4\right)}$$

$$\dot{x}_3 = \frac{s_{0_1}\alpha_1 F_{0_1} - s_{u_1}x_3}{1 + p_1x_1 - s_{v_1}q_1x_3} u_1 + \frac{\left(b_1x_1 - s_{v_1}a_1x_3\right) r x_6}{L_{01}\left(1 + p_1x_1 - s_{v_1}q_1x_3\right)}$$

$$\dot{x}_4 = \frac{s_{0_2}\alpha_2 F_{0_2} - s_{u_2}x_4}{1 + p_2x_2 - s_{v_2}q_2x_4} u_2 - \frac{\left(b_2x_2 - s_{v_2}a_2x_4\right) L_0L_{ii}\sin(x_5)}{L_{02}\sqrt{L_0^{\,2} + L_{ii}^{\,2} + 2L_0L_{ii}\cos(x_5)}\left(1 + p_2x_2 - s_{v_2}q_2x_4\right)} \tag{10}$$

$$\dot{x}_5 = x_6$$

$$\dot{x}_6 = \frac{1}{I}\left(x_3 r - x_4 \frac{L_0L_{ii}\sin(x_5)}{\sqrt{L_0^{\,2} + L_{ii}^{\,2} + 2L_0L_{ii}\cos(x_5)}} - mg\cos(x_5)\beta L_1 - K_e x_5 - F_v x_6 \right)$$

2.3 Model parameters identification

The parameters of the biomechanical system have been identified based on different protocols. The geometric parameters such as the insertion points, the muscle lengths, the moment arms, etc., were identified based on the Hawkins model (Hawkins & Hull, 1990) and using the Levenberg-Marquardt (Levenberg, 1944) algorithm. The knee joint dynamic parameters such as the joint stiffness and viscosity were identified through linear least square algorithm (Gautier & Poignet, 2002). Some muscle parameters such as the maximal muscle force and the force-length relationship were identified using non-linear interpolation. Other muscle parameters not yet identified on humans were taken from literature (El-Makssoud et al., 2004-a), basically the muscle stiffness and the contractile-elastic muscle length distribution.

2.3.1 Knee joint parameters identification

Kinematics data for the knee joint were measured through a motion analysis system and using the passive pendulum test. This test consists in recording the knee joint angle and velocity during a passive movement. The table 1 summarizes the identified knee joint parameters for a given subject. These parameters correspond respectively to the thigh length L_0, the quadriceps moment arm r and the two muscles insertion points L_{iq} and L_{ii} and their standard deviation. The hamstrings moment arm is position dependent (Eq. 4).

Parameter	L_0	r	L_{iq}	L_{ii}
Value (m)	0.3726	0.0397	0.0401	0.0648
Standard deviation (%)	0.335	3.230	3.138	0.441

Table 1. Knee joint parameter identification.

The parameters shown above, have been satisfactory identified and close to those found in literature (Kromer, 1994). The standard deviations were less than 4%. We can notice that the chosen movement trajectories excite sufficiently the unknown parameters. Figure 1 shows the muscle length computed by the Hawkins model and the model described above (Eq. 1, 2).

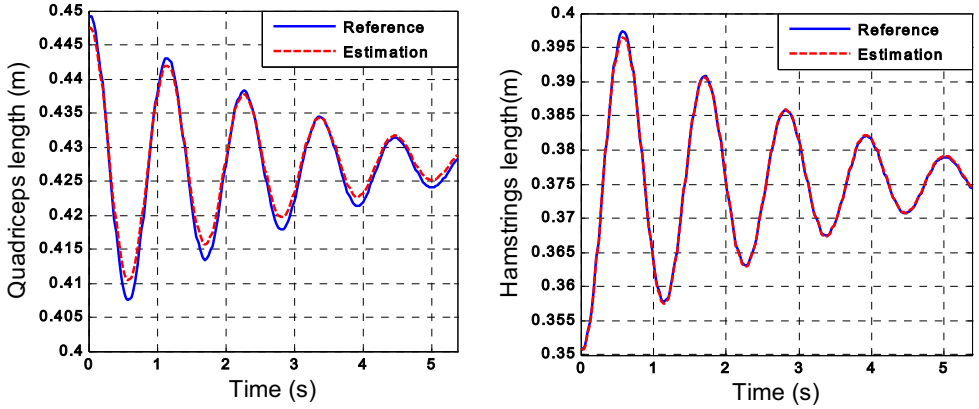

Fig. 4. Cross validation after parameter estimation (data not used during identification processing).

The dynamic parameters of the knee joint such as the knee stiffness and the knee viscosity were identified based on the following equation and using the linear least square method:

$$I\ddot{\theta} = -mgl\cos(\theta) - K_e\theta - F_v\dot{\theta} \tag{11}$$

We should notice that during a passive movement, the active moment produced by the muscles is equal to zero. Different subjects (healthy and paralyzed) have participated in the identification process. This latter was performed with the subject laying semi-supine with the lower legs hanging over the edge of a chair (Fig. 5). The operator raised the shank of the subject to given angle (about 45°) and leave the shank to swing freely until it reached the resting position (90°). The movement was recorded using a video based on motion analysis system (Vicon). Passive markers were fixed on the hip, knee and ankle (Fig. 5-b, 5-c). Kinematic data were acquired at 50 Hz sampling rate. In this application only three markers were sufficient to compute the knee joint angle and velocity. This system has the advantage to not overwhelming the subject by an external sensor that could affect the accuracy of the identification. Several tests were performed for each subject. The EMG signal analysis of the main muscles (quadriceps and hamstrings), serves only to identify any undesired voluntary muscle contractions and then reject the trial.

Fig. 5. a) Vicon system – b) Healthy subject - c) Paraplegic patient.

The anthropometric parameters such as the shank mass and inertia were estimated by using the regression equation proposed by DeLeva and Zatsiorsky (DeLeva, 1996), and by measuring the weight and the height of each subject. The anthropometric parameters of the subjects who participated in the identification are shown in table 2.

Subject	I (Kg.m^2)	m (Kg)	l (cm)
Healthy	0.1682	4.8852	19.46
Paraplegic 1	0.1536	4.5830	19.2
Paraplegic 2	0.2092	5.6162	20.26

Table 2. Estimation of the anthropometric parameters (Inertial moment, mass and length).

The dynamic parameters of the knee joint such as viscosity and stiffness were identified by means of linear least square methods (Gautier & Poignet, 2002). The knee angle position was extracted from the kinematic data, while velocity and acceleration were computed by numeric derivation using a low-pass filter. The identified parameters as well as their standard deviation (sd) are shown in table 3. These results could be compared to some results in literature (Ferrarin et al., 2001), computed in the same context.

Subject	F_v (N.m.s/rad)	sd (%)	K_e (N.m/rad)	sd (%)
Healthy	0.0838	6.4845	0.17	2.266
Paraplegic 1	0.0659	13.3589	0.1095	6.0050
Paraplegic 2	0.0897	10.6973	0.0529	10.1739

Table 3. Dynamic parameter identification.

2.3.2 Muscle parameters identification

The force-length relation (Riener & Fuhr, 1998) expressed by equation (Eq. 12) as well as the maximal isometric force that could be generated by a muscle were identified using a special experimental platform (Fig. 6)(Mohammed 2006). This latter is equipped by a force sensor, position sensor, a mechanical shank and foot blocking system, allowing force and position measurements during isometric stimulation tests.

$$F(L) = \exp\left[-\left(\frac{\bar{l}-1}{b_l}\right)^2\right] \tag{12}$$

Where $\bar{l} = \frac{L}{L_0}$, L is the muscle length and L_0 the muscle length at the rest position . b_l could be easily identified based on equation (Eq. 12).

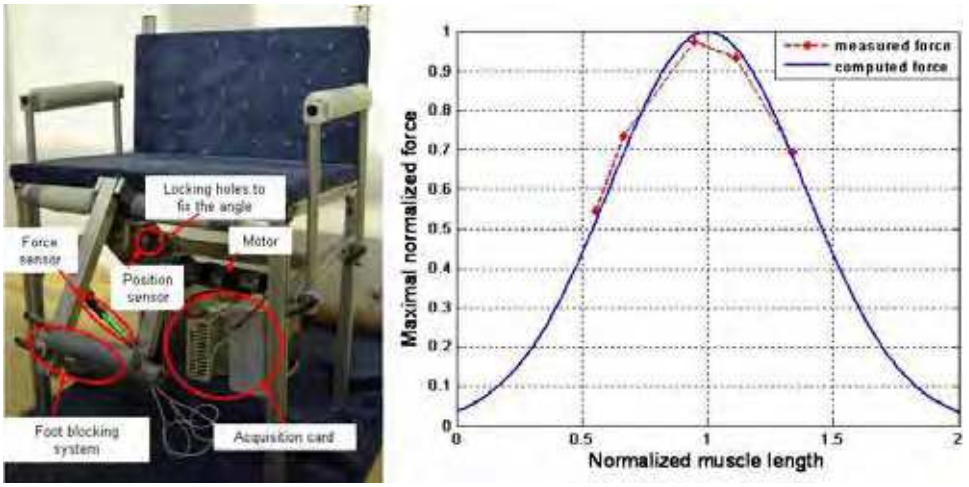

Fig. 6. Experimental platform and muscle parameter identification.

The muscle stiffness and the contractile-elastic muscle length distribution as shown in table (4), were taken from (El-Makssoud et al., 2004-a).

Muscle model parameters	Variable	quadriceps	hamstrings	Unit
Stiffness of the serial element E_s	K_s	1.10^4	1.10^4	N/m
Contractile element length E_c	L_{co}	41.10^{-2}	38.10^{-2}	m
Elastic element length E_s	L_{so}	8.10^{-2}	10.10^{-2}	m

Table 4. Parameters of both muscles: quadriceps and hamstrings

3. Sliding mode control

The nonlinearities of the muscle model and the required robustness regarding parameter variations and external disturbances lead us to adopt a controller relying on the sliding mode theory. This latter became recently widely used due to its high accuracy and robustness with respect to parameters' uncertainty and external disturbances. The control task is to keep a constraint, given by equality of a smooth function called sliding surface, equal to zero. The dynamic smoothness in the vicinity of the sliding surface represents the sliding order of the system. In this study, the goal was to control the muscles-knee biomechanical system under FES by means of high order sliding mode controller (HOSM) (Fridman, & Levant, 2002). The HOSM generalizes the basic sliding mode approach by acting on the higher order time derivatives of the sliding variable instead of influencing the first time derivative as it happens in the standard sliding mode control or first order sliding mode. Consequently, the discontinuity of the control vector does not appear in the first (r-1)th total time derivative (Eq. 13,14). The HOSM has the potential to provide greater accuracy and decrease the chattering phenomenon. A 2-sliding mode control may provide up to second order of sliding precision with respect to measurement interval. In this application, a state model of the knee with two antagonist muscles was derived. Here, the term antagonist will be used for muscles, whose moment in a two-dimensional system about a joint is in the opposite direction as the resulting joint moment. The antagonistic function of a muscle is not necessarily restricted to oppose motion but may give stability and stiffness to a joint. Unknown perturbations were added to the muscle forces generated in order to study the accuracy and robustness of the controller under external disturbances.

$$\frac{\partial s^{(i)}}{\partial \mathbf{u}} = 0, \quad (i = 1, 2, \ldots, r-1), \quad \frac{\partial s^{(r)}}{\partial \mathbf{u}} \neq 0 \tag{13}$$

$$s = \dot{s} = \ddot{s} = \ldots = s^{(r-1)} = 0 \tag{14}$$

Where s, r and **u** represent respectively the sliding surface, the relative degree and the resulting control vector.

3.1 Position control law strategy

The sliding surface used to constraint the dynamic behaviour of the biomechanical model is a first order differential equation chosen as:

$$s = \left(\dot{\theta}_d - \dot{\theta}\right) + \lambda\left(\theta_d - \theta\right) \tag{15}$$

Where $\dot{\theta}_d$ and θ_d are respectively the desired velocity and position, λ is a positive coefficient. Higher values of λ, lead to a faster convergence along the sliding surface to the zero point of the phase-plane. Let us consider the sliding surface (Eq. 15) in order to determine the relative order of the controlled system. We obtain the following result:

$$\frac{\partial \dot{s}}{\partial \mathbf{u}} = 0, \quad \frac{\partial \ddot{s}}{\partial \mathbf{u}} \neq 0 \tag{16}$$

Therefore, the relative degree of the sliding mode control is r = 2. Considering the step response case ($\ddot{\theta}_d$ = $\dot{\theta}_d$ = 0), the second order time derivative of the sliding surface can be written as:

$$\ddot{s} = -\ddot{x}_6 - \lambda \dot{x}_6 \tag{17}$$

The expression of the second order time derivative of the state variable x_6 is given by:

$$\ddot{x}_6 = \frac{1}{J}\begin{pmatrix} \dfrac{rS_{0_1}\alpha_1 F_{01}}{1+p_1x_1-s_{v_1}q_1x_3}u_1 - \dfrac{rs_{u_1}x_3}{1+p_1x_1-s_{v_1}q_1x_3}u_1 + r\dfrac{\left(b_1x_1-s_{v_1}a_1x_3\right)rx_6}{L_{01}\left(1+p_1x_1-s_{v_1}q_1x_3\right)} \\ -\dfrac{s_{0_2}\alpha_2 F_{02}L_0L_{ii}\sin\left(x_5\right)}{\left(1+p_2x_2-s_{v_2}q_2x_4\right)\sqrt{L_0^{\,2}+L_{ii}^{\,2}+2L_0L_{ii}\cos\left(x_5\right)}}u_2 + \dfrac{s_{u_2}x_4L_0L_{ii}\sin\left(x_5\right)}{\left(1+p_2x_2-s_{v_2}q_2x_4\right)\sqrt{L_0^{\,2}+L_{ii}^{\,2}+2L_0L_{ii}\cos\left(x_5\right)}}u_2 \\ -\dfrac{\left(b_1x_1-s_{v_1}a_1x_3\right)rX_6L_0L_{ii}\sin\left(x_5\right)}{L_{01}\left(1+p_1x_1-S_{v_1}q_1x_3\right)\sqrt{L_0^{\,2}+L_{ii}^{\,2}+2L_0L_{ii}\cos\left(x_5\right)}} - x_4\dfrac{L_0L_{ii}x_6\cos\left(x_5\right)\sqrt{L_0^{\,2}+L_{ii}^{\,2}+2L_0L_{ii}\cos\left(x_5\right)}}{L_0^{\,2}+L_{ii}^{\,2}+2L_0L_{ii}\cos\left(x_5\right)} \\ -X_4\dfrac{L_0^{\,2}L_{ii}^{\,2}\sin^2\left(x_5\right)}{\left(L_0^{\,2}+L_{ii}^{\,2}+2L_0L_{ii}\cos\left(x_5\right)\right)\sqrt{L_0^{\,2}+L_{ii}^{\,2}+2L_0L_{ii}\cos\left(x_5\right)}} + mg\beta L_1x_6\sin(x_5) - K_ex_5 - F_vx_6 \end{pmatrix} \tag{18}$$

Inserting the expressions of $\dot{x}_6$ and $\ddot{x}_6$ within equation (Eq. 17) allows writing the second order time derivative of the sliding surface as:

$$\ddot{s} = \varphi(\mathbf{x},\mathbf{t}) + \gamma(\mathbf{x},\mathbf{t})\mathbf{u} \tag{19}$$

It is assumed that $|\varphi| \le \Phi$, $0 < \Gamma_m \le \gamma \le \Gamma_M$ (Levant, 1993), where Γ_m, Γ_M and Φ are positive constants. We express the equation (Eq. 19) as:

$$\begin{cases} \dot{y}_1 = y_2 \\ \dot{y}_2 = \varphi(\mathbf{x},\mathbf{t}) + \gamma(\mathbf{x},\mathbf{t})\mathbf{u} \end{cases} \tag{20}$$

Where $y_1 = s$. In that case, the problem is equivalent to the finite time stabilization problem for a second order system.

3.2 Statement of the control algorithm

(Levant, 1993) presented a range of 2-sliding algorithms to stabilise second order uncertain nonlinear systems. In the current study we implemented the algorithm with prescribed law of variation of the sliding surface. This choice has been made based on criteria of relative robustness and finite time convergence (Fridman, & Levant, 2002). The general formulation of such a class of a sliding mode control algorithm is:

$$\dot{u} = \begin{cases} -u & if\ |u| > 1 \\ -V_M\, sign(y_2 - g_c(y_1)) & if\ |u| \le 1 \end{cases} \tag{21}$$

Where V_M is a positive constant and g_c a continuous function (Fig. 7) as given by Eq. 22. Moreover, this function must verify some specific conditions (Fridman, & Levant, 2002).

$$g_c\left(y_1\right) = -\lambda_1\left|y_1\right|^{\rho} sign\left(y_1\right), \quad \lambda_1 > 0, \quad 0.5 < \rho \le 1 \tag{22}$$

The sufficient condition for the finite time convergence to the sliding manifold is defined by the following inequality:

$$V_m > \frac{\Phi + \sup\left[\dot{g}_c(y_1)g_c(y_1)\right]}{\Gamma_m} \tag{23}$$

Larger values of λ_1 accelerate the convergence to reach the sliding surface and provide better robustness and stability. A substitution of y_2 by Δy_1 is theoretically possible if y_2 is not available.

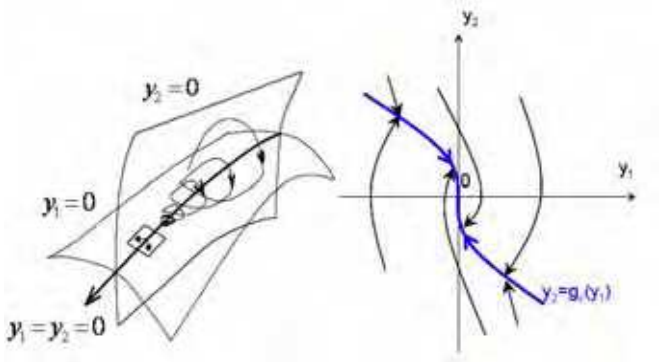

Fig. 7. Phase plot of the prescribed convergence law algorithm (Levant, 1993).

3.3 Simulation results

We have implemented the control algorithm defined by equation (Eq. 21) on the simulator of the knee-muscle biomechanical model (cf. Eq. 10). The components of the control vector **u** are the chemical inputs (u_q, u_h) and the ratio of the recruited fibers (α_q, α_h). These coefficients depend on sliding mode controller output. In our case, the knee joint is controlled by two muscle's groups: quadriceps and hamstrings. Consequently, there are two electrical currents, I_q and I_h as well as two Pulse Width Modulation values, PW_q and PW_h which have to be deduced from the sliding mode control variable u (Mohammed, et al. 2005). According to the sign of the resulting control variable at the output of the HOSM *c*ontroller, we have chosen to stimulate either the quadriceps or the hamstrings (Eq. 25).

$$u = -\int V_M sign(y_2 - g_c(y_1))\,dt \qquad (\text{if } |u| \le 1) \tag{24}$$

$$\text{If } (u > 0) \Rightarrow \begin{cases} I_q = \dfrac{u}{u_{nom}} I_{\max} \\ I_h = 0 \end{cases} \qquad \text{If } (u < 0) \Rightarrow \begin{cases} I_q = 0 \\ I_h = \dfrac{u}{u_{nom}} I_{\max} \end{cases} \tag{25}$$

Where, u_{nom} and I_{max} represent respectively the nominal value of the sliding control variable u and the maximal value authorized to stimulate a muscle (around 200 mA). The current values for quadriceps I_q and hamstrings I_h and/or the Pulse Width, respectively PW_q and PW_h enable us to evaluate the required ratios of fibers to be recruited (α_q, α_h). The chemical inputs u_q and u_h are automatically activated when the electrical currents are respectively superior to zero. We have implemented this algorithm on a simulator built with the Matlab-Simulink environment. In the following simulations, we have applied two different knee desired positions, starting from the rest position, $\theta_d = 90^\circ$ as:

$$\begin{cases} 1)\quad 1s < t < 4s : \theta_d = 130^\circ \\ 2)\quad 6s < t < 9s : \theta_d = 50^\circ \\ 3)\quad \text{Otherwise} : \theta_d = 90^\circ \end{cases} \tag{26}$$

The coefficients of the 2-sliding controller were chosen to verify the condition equations (Eq. 23). The following values have been used: $\lambda = 10$, $\lambda_1 = 20$, $\rho = 0.7$, $V_M = 1$. Figure 8-a shows the step response for different desired values. Desired and current angle curves match when sliding surface reaches zero. As we can notice, the dynamic of the system is constrained to the dynamic of the sliding surface. The finite time convergence of the sliding surface is about 1sec in knee flexion and extension (Fig.8-b). In Fig.9-a, we present the resulting stimulation currents for both quadriceps and hamstrings I_q and I_h. The control vector **u** computed by the equation (Eq. 24) is shown in Fig.9-b.

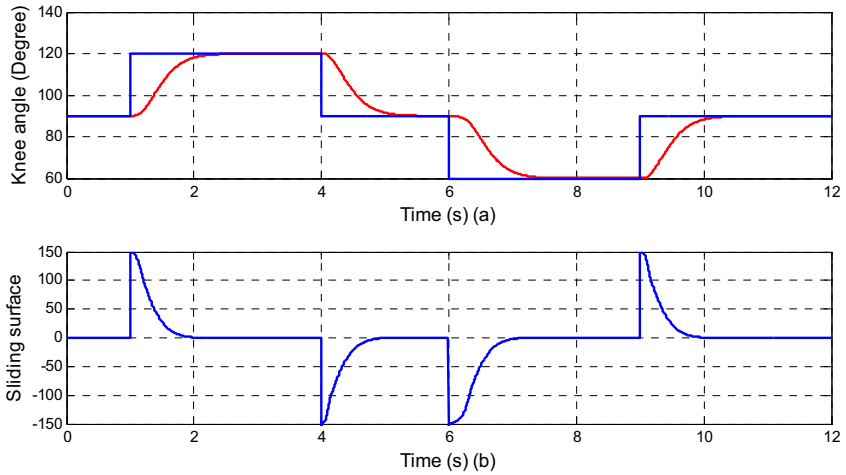

Fig. 8. a) Desired step and actual knee angle variation, b) Stabilization of the sliding surface.

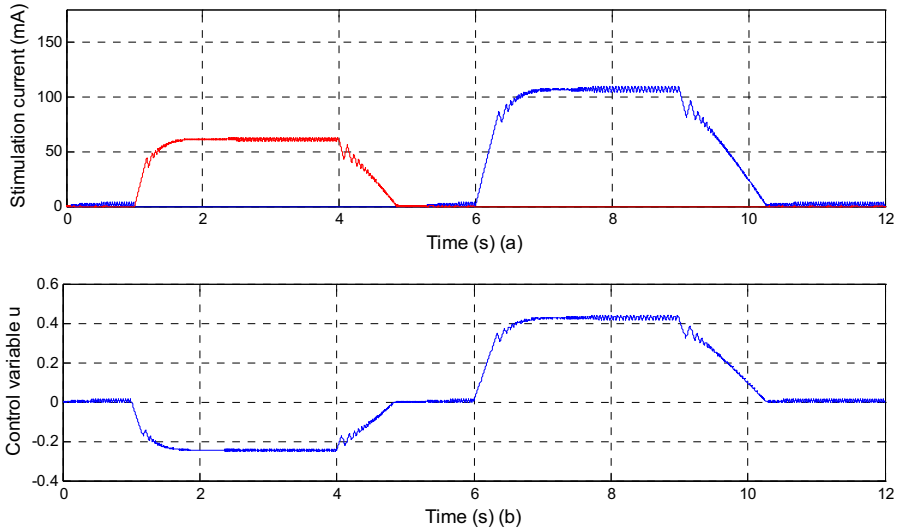

Fig. 9. a) Stimulation currents of both muscles, b) The control vector u.

4. Model predictive control MPC

The ability to handle nonlinear multi-variable systems that are constrained in states and/or control variables motivates the use of Model Predictive Control (MPC), (Allgöwer et al., 1999). This approach proved its efficiency in a large variety of industrial processes, especially in chemical processes. The MPC problem is usually stated as an optimization one subject to physical coherent constraints, and is solved with classical optimization algorithms. The MPC has been widely used in different applications due to their interesting properties (Camacho & Bordons, 1995). In our particular case, the nonlinearities of the muscle model, the constraints on the input stimulation current and on the output knee joint position lead us to adopt a controller relying on MPC. Few studies applied this technique to a musculoskeletal system. Some authors have used MPC with black-box models instead of continuous time physiological models (Schauer & Hunt, 2000).

4.1 Problem formulation

The MPC problem is usually formulated as a constrained optimization problem, (Allgöwer et al., 1999):

$$\min_{u_k^{H_p}} J(x_k, u_k^{H_p})$$

subject to:

$$\begin{aligned} u_{i|k} &\in U, \quad i \in [0, H_u] \\ x_{i|k} &\in X, \quad i \in [0, H_p] \end{aligned} \tag{27}$$

where

$$U := u_k \in \mathrm{R}^m \mid u_{\min} \le u_k \le u_{\max}$$
$$X := x_k \in \mathrm{R}^m \mid x_{\min} \le x_k \le x_{\max}$$

Internal controller variables predicted from time instance k are denoted by a double index separated by a vertical line where the second argument denotes the time instance from which the prediction is computed. $x_k = x_{0|k}$ is the initial state of the system to be controlled at time instance k and: $\hat{u}_k = \left[u_{0|k}, u_{1|k}, \ldots u_{H_u-1}, u_{H_u-1}, \ldots u_{H_u-1} \right]$ an input vector of dimension H_p (prediction horizon). At each sample, a finite optimal control problem is solved over the prediction horizon. We assume that we would like the controlled variables, y_k (Fig.10), to follow some reference trajectory r. Predictive control consists in computing the vector $\hat{u}_k$ of consecutive inputs $u_{i|k}$ over the control horizon H_u by optimizing the objective function J under given constraints (Eq. 27). The control signal is assumed to be constant after H_u samples over a horizon of $(H_p - H_u)$ dimension. When the solution of the optimal control problem has been obtained, the value of the first control variable in the optimal trajectory, $u_{k|k}$, is applied to the process. The rest of the predicted control variable trajectory is discarded, and at the next sampling interval the entire procedure is repeated (Kesson, 2003). These computations are updated at each sampling time.

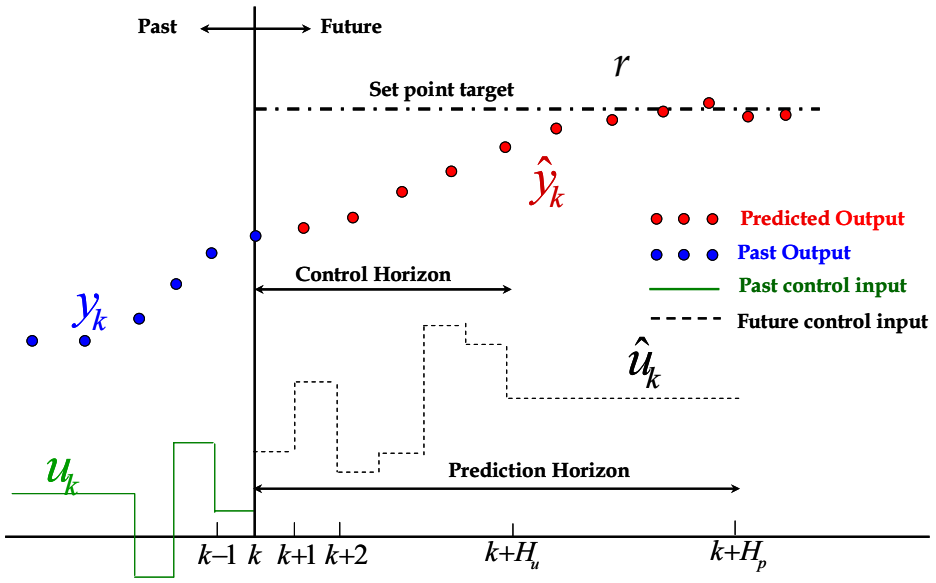

Fig. 10. Principles of the predictive control strategy design (Seborg et al., 2004).

The nonlinear equality constraint on the state represents the dynamic model of the system. Bounding constraints over the inputs $u_{i|k}$ and the state variables $x_{i|k}$ over the prediction horizon H_p are defined through the sets U and X (Eq. 27). The objective function J is usually defined as:

$$J(x_k, u_k^{H_p}) = \phi(x_{H_p|k}) + \sum_{i=0}^{H_u} L(x_{i|k}, u_{i|k}) \tag{28}$$

where Φ is a constraint on the state at the end of the prediction horizon, called state terminal constraint, and L a quadratic function of the state and inputs. The computation of the solution $u_k^{H_p}$ can be divided in two steps: firstly, computation of a solution satisfying the constraints (including the state terminal constraint), and secondly optimization. The first step involves bounding constraints (Eq. 27), and nonlinear constraints expressing the dynamic model of the system (Eq. 9). Simulations were performed in Matlab-Simulink environment using the "ode45" integration algorithm with variable step size. The simulation codes were adapted from MPCtools, (Kesson, 2003).

4.2 Model Linearization

The system (Eq. 9) is a nonlinear multivariable system. In a first step and in order to apply a linear predictive controller, we made some assumptions to the nonlinear system. The goal was to get a feasible solution before applying the controller to the non linear plant. Some hypotheses make this nonlinear system easier:

- We consider that the chemical control u_{ch} is a positive constant indicating a muscular fiber fusion. This hypothesis could be justified in our case by the fact that the stimulation frequency is much greater then the muscular fiber fusion.

Consequently, during stimulation, we have only contractions and no relaxations:
$s_u = 1, \quad s_v = -1, \quad |u| = u, \quad |\dot{\varepsilon}_c| = -\dot{\varepsilon}_c$

- Only one muscle, the quadriceps has been taken into account in the following causing knee extension. When no extension, the gravity induces knee flexion to the rest position.
- We suppose that the stiffness of the serial element which represents the tendon is much greater than the stiffness of the contractile element. This hypothesis is true since we are performing only dynamic movements and no isometric stimulations were considered.

$$\dot{\varepsilon}_c = \frac{L_0}{L_{c0}}\dot{\varepsilon} - \frac{1}{L_{c0}K_s}\dot{F}_c$$

In the above conditions, the term $\frac{1}{L_{c0}K_s}\dot{F}$ is less than $10^{-3}\frac{L_0}{L_{c0}}\dot{\varepsilon}$

By taking into account the above assumptions, the plant model will have a reduced nonlinear form where $\mathbf{x} = [x_1\ x_2\ x_3\ x_4]^T = [K\ F\ \theta\ \dot{\theta}]^T$ is the state vector and $\mathbf{u} = \alpha$ is the control input. The plant model could thus be expressed by the following set of differential equations:

$$\begin{aligned}
\dot{x}_1 &= ax_1 + bx_1x_4 + cf_l(x_3)u \\
\dot{x}_2 &= dx_1x_4 + ax_2 + bx_2x_4 + ef_l(x_3)u \\
\dot{x}_3 &= x_4 \\
\dot{x}_4 &= fx_2 + h\cos(x_3) + lx_4
\end{aligned} \tag{29}$$

Where:

$$a = -u_{ch}, b = \frac{r}{L_{c0}}, c = u_{ch}K_0, d = -r, e = u_{ch}F_0$$

$$f = \frac{r}{I}, h = \frac{-mg\beta L_1}{I}, l = \frac{-F_v}{I}, f_l = \exp\left[-\left(\frac{\bar{l}-1}{b_l}\right)^2\right]$$

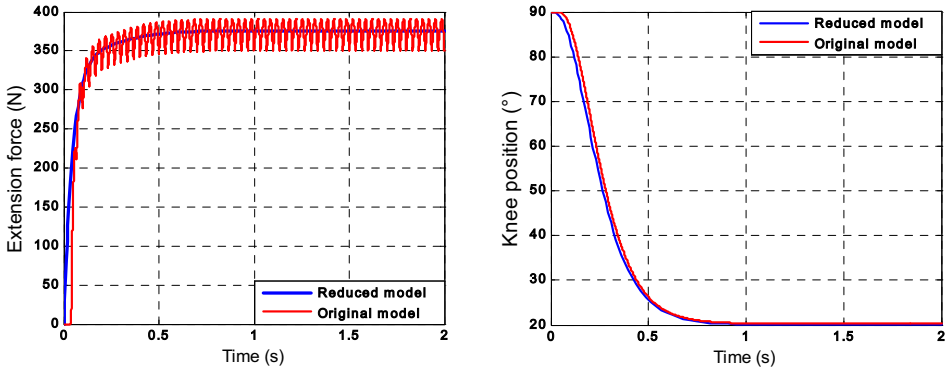

Fig. 11. Non linear models: original and reduced.

The above hypotheses were validated through simulations as shown in figure (11). This latter presents the responses of both, the original non linear model (Eq. 9) and the reduced non linear model (Eq. 29). On the left side, we show the force generated by both models. The original non linear model presents some oscillations reflecting the contraction-relaxation cycle. These oscillations results from the stimulation frequency. On the right side of figure (11), we present the knee position output of both models. We can notice that the linearized model fits well with the original one in terms of force generation as well as knee angular position. A linearization of this system around an arbitrary operating point $(\bar{\mathbf{x}}, \bar{\mathbf{u}})$ has been computed using its Jacobian. The linear model could be formulated as follows:

$$\begin{cases} \dot{\mathbf{x}} = \mathrm{A}\,\mathbf{x} + \mathrm{B}\,\mathbf{u} \\ \mathbf{y} = \mathrm{C}\,\mathbf{x} + \mathrm{D}\,\mathbf{u} \end{cases} \tag{30}$$

Where:

$$\mathrm{A}=\begin{bmatrix} a+b\bar{x}_4 & 0 & c\bar{u}\,\dot{f}_l(\bar{x}_3) & b\bar{x}_1 \\ d\bar{x}_4 & a+b\bar{x}_4 & e\bar{u}\,\dot{f}_l(\bar{x}_3) & d\bar{x}_1+b\bar{x}_2 \\ 0 & 0 & 0 & 1 \\ 0 & f & -h\sin(\bar{x}_3) & l \end{bmatrix} \quad \mathrm{B}=\begin{bmatrix} c\bar{u}\,f_l(\bar{x}_3) \\ e\bar{u}\,f_l(\bar{x}_3) \\ 0 \\ 0 \end{bmatrix} \quad \mathrm{C}=\begin{bmatrix} 0 & 0 & 1 & 0 \end{bmatrix} \quad \mathrm{D}=0$$

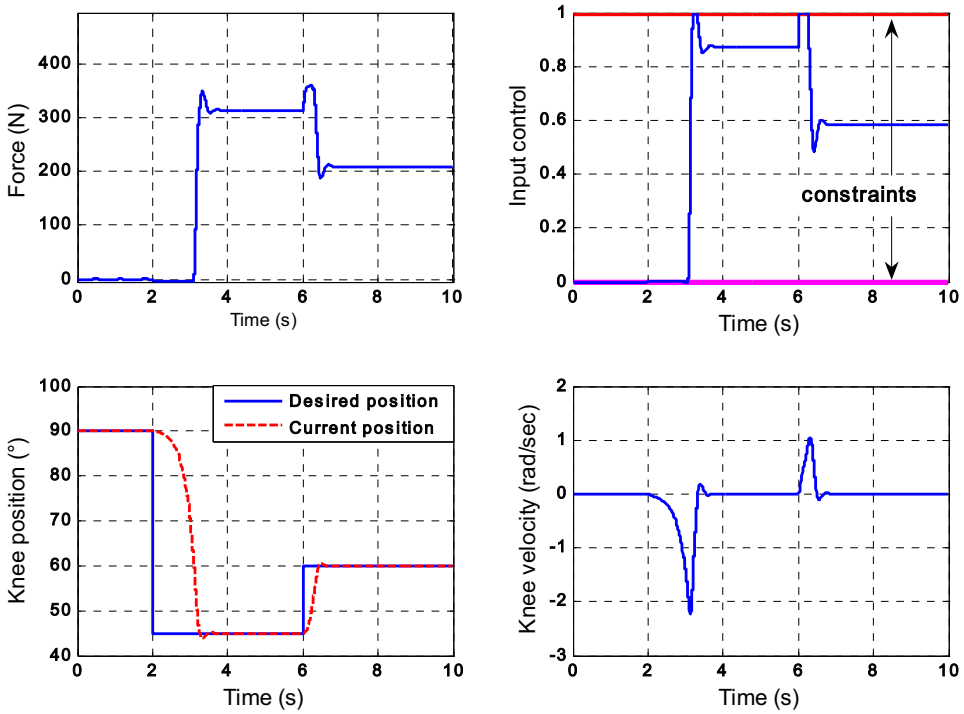

Fig. 12. Tracking knee joint trajectory and controller performance.

4.3 Simulation results (MPC)

Different simulation tests have been carried out. The sample period was set to 0.01 sec, the prediction and control horizon H_p and H_u were computed as a function of the system time constant: H_p =30 and H_u =10. The constrained input u = α was the recruitment variable. Since the recruitment function is static, the optimal pulse width or stimulation amplitude could be easily computed. The recruitment variable has been constrained to be between 0 and 1 representing respectively no fiber recruited and full recruitment. The controlled variable, which is the system output, was constrained to stay between θ = 0° (hyperextension) and θ = 90° (resting position). Only the knee angle was used as feedback to update the control input. Controller parameters were calculated offline. Simulation results are shown in figures 12, 13 and 14.

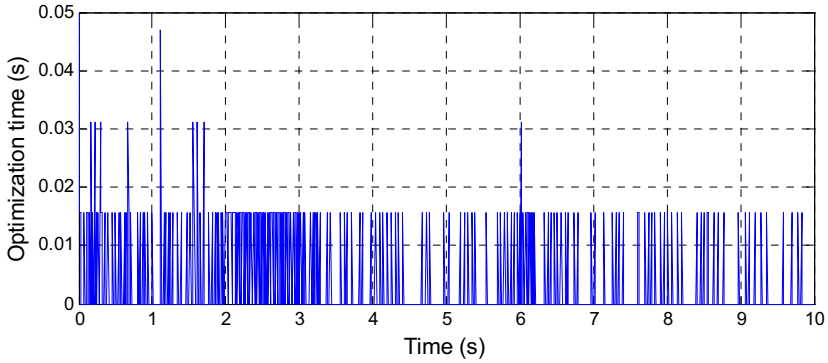

Fig. 13. Predictive control optimization time.

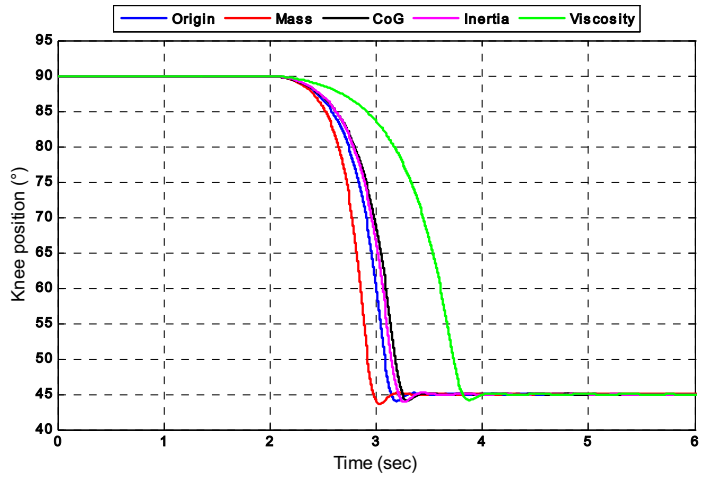

Fig. 14. MPC robustness: uncertainty on mass, position of the centre of gravity, inertia and viscosity.

In figure (12), initial conditions correspond to θ =90°, which means the knee joint is in the rest position. After 2 seconds, the desired trajectory was stepped to θ = 45° which corresponds to medial knee extension. The controller converges to the desired position in a

finite time while maintaining the control input between its limits. At time = 6 s, we perform a 15° knee flexion inducing a muscle force and stiffness decrease. The controller managed to converge to the desired position and to fully compensate the position change without need for any feedback observer and respecting at the same time the constraints on input and output. Figure (13) shows the optimization time needed to perform the above simulation. It should be noticed that the muscle parameters used in these simulation relate to a healthy subject (Tables 2 and 3). The inaccuracy that may occur on these parameters when dealing with paraplegic patients could be compensated by the robustness of the (MPC) controller. In figure (14), we studied the controller robustness against parameter variations. In fact, the uncertainty could affect mainly the inertial parameters which have been estimated, based on statistical abacuses and regression equations (De Leva, 1996). Although the parameters uncertainties imposed were relatively important (20% - 25%) from the initial value, the MPC controller showed a satisfactory robustness regardless these uncertainties.

5. Controllers performance – comparative study

In this section, we have drawn a comparison between the controllers' performance (HOSM and MPC) in terms of input control and state regulation. These controllers were simulated under the same conditions. A classical linear controller based on poles placement (PP) serves as a reference controller.

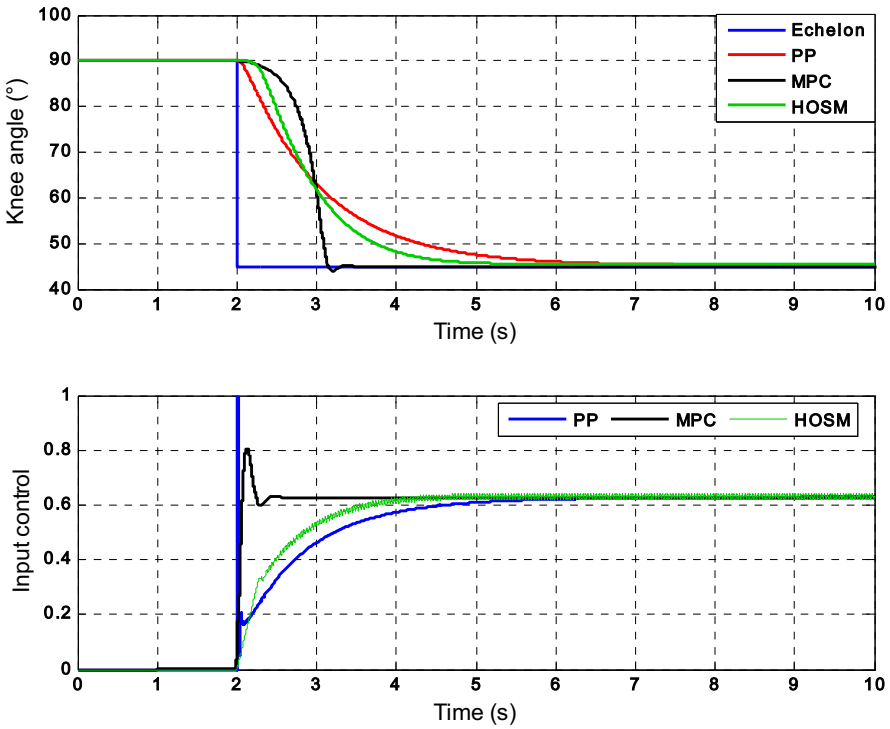

Fig. 15. Comparison of control strategies: desired position corresponds to 45° knee extension. PP for poles placement, MPC for predictive control and HOSM for high order sliding mode.

In figure (15), we have simulated a 45° knee extension by activating the quadriceps muscle. Unlike the PP controller which takes the longest time to converge to the desired position and presents at the same time an input saturation during the transient period, the MPC controller converged to the desired position in a relatively limited time. Saturation of the input control means an important rate of stimulation firing during the transient period. The HOSM controller shows a satisfactory performance in terms of time convergence and position regulation. We can notice that the system dynamics evolution is constrained to the sliding surface dynamic (Eq. 15). Input control does not show also any overshoot, and the chattering effect has been considerably reduced. In order to study the robustness of these controllers, we have induced a position perturbation that corresponds to a quick and limited knee flexion. In terms of position regulation figure (16) shows that the different controllers succeed to converge to the desired position. In terms of input control, the PP controller is very sensitive to this perturbation; the MPC controller is much less sensitive and finally the HOSM controller that showed the best performance against external perturbation.

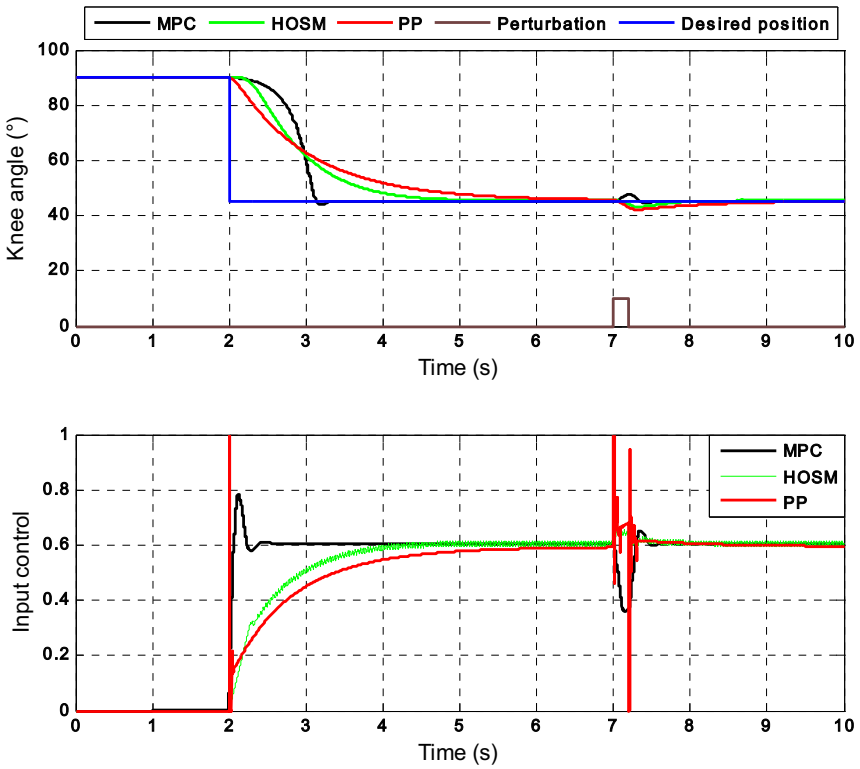

Fig. 16. Controllers behaviors against an external perturbation.

6. Conclusion

The main challenge that we face when applying FES to the paralyzed lower limbs is to avoid hyperstimulation and to defer the muscular fatigue as much as possible. Few

studies have treated the human muscle as an entire physiological element in a closed loop system. Known by their robustness against unknown perturbation and their accuracy against model mismatch, we have used robust control techniques such as the High Order Sliding mode (HOSM) and the Model Predictive Control (MPC) in a closed loop control scheme. The MPC offers the possibility to integrate constraints on input, output and measured states explicitly in its formulation. These strategies have ensured, by simulations, a robust control and a safer movement of the paralysed lower extremities. The controllers were applied to a multi-scale muscle model developed within the *DEMAR* project and recently published (El-Makssoud et al., 2004 -a). It is based on internal physiological characteristics assembling two levels: the microscopic one, involving the sliding actin-myosin filaments and the macroscopic part represented by a contractile element and an elastic element. This highly non linear model has been described by a set of differential equations. We have made some realistic assumptions to the biomechanical model of the knee joint actuated by two groups of antagonistic muscles (quadriceps and hamstrings). As a result we obtained a simplified nonlinear version of the knee-muscle formulation. Dynamic and geometric parameters were identified based on experimental kinematics data recorded using a video based motion analysis. Different identification techniques were applied such as the least square, non-linear interpolation, regression equations, etc. We were able to control the quadriceps-hamstrings muscles for the knee flexion-extension in order to track a predefined position trajectory within a large range of movement. Satisfactory stability and tracking error were achieved after a finite time delay. The performance of the closed loop system has been assessed in the presence of external force perturbations. Controller responses to these perturbations vary from the most sensitive (PP) to the MPC controller and finally the HOSM controller which seemed to be the most robust against external perturbations. We should notice that the system dynamic was constrained to follow the sliding surface dynamics. The MPC had shown a better performance in terms of time response than the HOSM. The results show that we respect the constraints on input and output. We are trying to limit the computational effort which is a common deficit of the MPC design. Actually, the optimisation time obtained (Fig.13) is around 20 ms in Matlab environment which is quite encouraging for a real time implementation. Experiments are ongoing to validate the control scheme on paraplegic patients by using the multi-moment platform used during the identification protocol (Fig. 6).

7. References

Allgöwer, F.; Badgwell, T.A.; Qin, S.J.; Rawlings, J.B. & Wright, S.J. (1999). Nonlinear predictive control and moving horizon estimation - an introductory overview, *In: Frank, P.M (edt.), Advances in control: highlights of ECC'99*, Springer, (1999), p. 391-449.

Bajd, T.; Kralj, A.; Sega J.; Turk R.; Benko H. & Strojnik, P. (1981). Use of a two- channel functional electrical stimulator to stand paraplegics, In: *Physical therapy*, 61(4), p.526-7.

Camacho, E. & Bordons, C. (1995). Model Predictive Control in the Process Industry *Springer-Verlag New York, Inc.*

DeLeva, P., (1996) Adjustments to zatsiorsky-seluyanov's segment inertia parameters. *Journal of Biomechanics*, Vol.29, p.1223-1230.

Donaldson, N. & Yu, C. (1996). FES standing control by handle reactions of leg muscle stimulation (CHRELMS), *IEEE Transactions on rehabilitation engineering*, 4(4) p.280-284.

El-Makssoud, H.; Guiraud, D. & Poignet, P. (2004-a). Mathematical muscle model for Electrical Stimulation control strategies, *IEEE International Conference on Robotics and Automation*, p. 1282-1287.

El-Makssoud, H.; Guiraud, D. & Poignet, P. (2004-b). Enhancement of physiological and mechanical modelling of the skeletal muscle controlled by Functional Electrical Stimulation. *International Functional Electrical Stimulation Society (IFESS),* Bournemouth, UK 6-9 September 2004.

Ferrarin, M.; Palazzo. F & Riener R. (2001). Model-Based Control of FES Induced Single Joint Movements, *IEEE Transactions on Neural systems and rehabilitation engineering*, 9(3), p.245-257.

Fridman, L. & Levant, A. (2002). High-Order Sliding Modes, *in: Sliding Modes Control in Engineering,* Ed. W. Perruquetti, J.P. Barbot, Marcel Dekker, Inc. New-York, p. 53-101.

Gautier, M. & Poignet P., (2002). Closed loop identification by inverse model of physical parameters of mechatronic systems. *Journal européen des systèmes automatisés*, Vol.36, No.3, p.465-480.

Hawkins, D. & Hull, M. (1990). A method for determining lower extremity muscle- tendon lengths during flexion/extension movements. *Journal of Biomechanics*, Vol. 23, p.487-494.

Kesson, J. (2003), Operator Interaction and Optimization in Control Systems, *P.hd thesis,* Department of Automatic Control Lund Institute of Technology.

Kromer, V. (1994). Analyse des forces musculaires au cours de la marche - Approche en corps rigide et simulation en mécanismes plans flexibles par éléments finis, *P.h.d. Thesis,* Institut national polytechnique de Lorraine (INPL).

Levant, A. (1993). Sliding order and sliding accuracy in sliding model control, *International Journal of Control*, Vol.58 No.6, p.1247-1263.

Levenberg, K. (1944). A method for the solution of certain problems in least square. *Quarterly applied Mathematics*, Vol. 2, p.164-168.

Mohammed, S.; Fraisse, P.; Guiraud, D.; Poignet, P. & H. El Makssoud, (2005-a). Robust Control Law Strategy Based on High Order Sliding Mode : Towards a Muscle Control, in: *IROS'05: International Conference on Intelligent Robots & Systems,* p. 2882-2887.

Mohammed, S. (2006), Contribution à la synthèse de movement et à la commande des muscles squelettiques sous Stimulation Electrique Fonctionnelle, *P.h.d. Thesis,* LIRMM-Université de Montpellier II.

Mulder, AJ.; Veltink, PH. & Boom, HB. (1992). On/off control in FES-induced standing up: a model study and experiments. *Medical and Biological Engineering and Computing*, 30(2), p. 205-212.

Poboroniuc, M.; Wood, D.; Donaldson, N.; Fuhr, T. & Riener R. (2003). Closed-loop control for FES-based restoration of standing in paraplegia, *2nd World Congress of the International Society of Physical and Rehabilitation Medicine-ISPRM*, Prague, Czech Republic, May 18-22, p.201-204.

Poboroniuc, M.; Fuhr, T.; Wood, D.; Riener, R. & Donaldson, N. (2002). FES-Induced Standing-Up and sitting down control strategies in Paraplegia", *FESnet Conference*. September 2nd-3rd, Glasgow, UK, p.1-3.

Riener, R. & Fuhr, T. (1998). Patient-Driven Control of FES-Supported standing Up: A simulation study, *IEEE Transactions on rehabilitation engineering*, 6(2), p.113-123.

Schauer, T. & Hunt, K.J., (2000). Nonlinear predictive control of knee-joint angle using FES, *International Functional Electrical Stimulation Society (IFESS),* Aalborg, Denmark, p. 425-428.

Seborg, D.E.; Edgar, T. F. & Mellichamp, D. A., (2004) Process Dynamics and Control, 2nd edition, John Wiley and Sons, New York.

Veltink, P.H.; Chizeck, H.J.; Crago, P.E. & El-Bialy, A. (1992). Nonlinear joint angle control for artificially stimulated muscle. *IEEE Transactions on biomedical engineering*, Vol. 39 N.4, p. 368-380.

Wood, DE.; Harper, VJ.; Barr, FMD.; Taylor, PN., Phillips, GF. & Ewins, DJ. (1998). Experience in Using Knee angles as part of a closed-Loop Algorithm to control FES-Assisted Paraplegic Standing, *6th Vienna International Workshop on Functional Electrostimulation,* (Vienna, Austria), p.137-140.

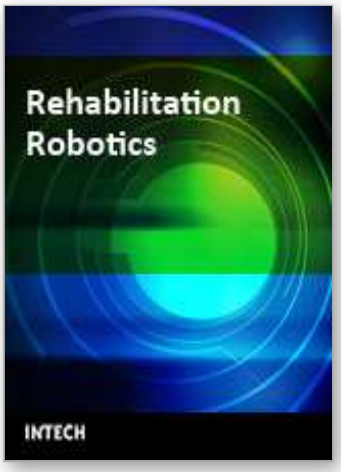

Rehabilitation Robotics

Edited by Sashi S Kommu

ISBN 978-3-902613-04-2
Hard cover, 648 pages
Publisher I-Tech Education and Publishing
Published online 01, August, 2007
Published in print edition August, 2007

The coupling of several areas of the medical field with recent advances in robotic systems has seen a paradigm shift in our approach to selected sectors of medical care, especially over the last decade. Rehabilitation medicine is one such area. The development of advanced robotic systems has ushered with it an exponential number of trials and experiments aimed at optimising restoration of quality of life to those who are physically debilitated. Despite these developments, there remains a paucity in the presentation of these advances in the form of a comprehensive tool. This book was written to present the most recent advances in rehabilitation robotics known to date from the perspective of some of the leading experts in the field and presents an interesting array of developments put into 33 comprehensive chapters. The chapters are presented in a way that the reader will get a seamless impression of the current concepts of optimal modes of both experimental and ap- plicable roles of robotic devices.

How to reference

In order to correctly reference this scholarly work, feel free to copy and paste the following:

Samer Mohammed, Philippe Poignet, Philippe Fraisse and David Guiraud (2007). Rehabilitation of the Paralyzed Lower Limbs Using Functional Electrical Stimulation: Robust Closed Loop Control, Rehabilitation Robotics, Sashi S Kommu (Ed.), ISBN: 978-3-902613-04-2, InTech, Available from: http://www.intechopen.com/books/rehabilitation_robotics/rehabilitation_of_the_paralyzed_lower_limbs_using_functional_electrical_stimulation__robust_closed_l

INTECH
open science | open minds

InTech Europe
University Campus STeP Ri
Slavka Krautzeka 83/A
51000 Rijeka, Croatia
Phone: +385 (51) 770 447
Fax: +385 (51) 686 166
www.intechopen.com

InTech China
Unit 405, Office Block, Hotel Equatorial Shanghai
No.65, Yan An Road (West), Shanghai, 200040, China
中国上海市延安西路65号上海国际贵都大饭店办公楼405单元
Phone: +86-21-62489820
Fax: +86-21-62489821